**Proceedings of PVP2008**
**2008 ASME Pressure Vessels and Piping Division Conference**
**July 27-31, 2008, Chicago, Illinois, USA**

**PVP2008-61349**

# MEASUREMENT OF INTERNAL STRAINS IN GRAPHITE USING THE DEEP HOLE DRILLING TECHNIQUE

**Soheil Nakhodchi**, Department of Mechanical Engineering, University of Bristol, Queen's Building, University Walk, Bristol, BS8 1TR

**Peter E J Flewitt,** H.H. Wills Physics Laboratory, University of Bristol, Tyndall Avenue, Bristol, BS8 1TL, UK

**Chris Truman,** Department of Mechanical Engineering, University of Bristol, Queen's Building, University Walk, Bristol, BS8 1TR

**David J Smith,** Department of Mechanical Engineering, University of Bristol, Queen's Building, University Walk, Bristol, BS8 1TR

## ABSTRACT

Currently, measurement of internal strains deep inside graphite is extremely difficult. As a consequence there is a need to assess the ability of a deep-hole drilling (DHD) method to measure internal strains in reactor core graphite and explore the potential for in-situ measurement. DHD technique is a semi-destructive method for measurement of the through thickness residual stresses. The technique previously has been applied successfully to metallic and composite materials. In this paper, the method for stress measurement in graphite is examined particularly when a significant volume fraction of porosity is present. Two types of graphite were used, PGA and PG25 filter graphite. In PGA graphite the Young's modulus of elasticity was orientation dependent. As a consequence samples were cut from blocks in two directions. PG25 filter graphite is a surrogate for service exposed material.

Known loads were applied to graphite beam samples and the DHD method was used to measure the stress/strain profile through the material. The results were compared with the strain data obtained from strain gauges bonded to the samples. Overall, there was an excellent agreement between the DHD measured stress/strain and applied stress. It is shown that deep-hole drilling technique can measure linear stress distributions in graphite.

## INTRODUCTION

The reactor cores of gas cooled reactors, both Magnox and Advanced Gas cooled Reactors, which are used in the UK are made from assemblies of bricks of polygranular graphite[1, 2]. Exposure of these reactor cores to the service environment of fast neutrons and hot $CO_2$ coolant gas results in irradiation hardening and radiolytic oxidation of the graphite during the service life. These effects lead to progressive changes in the physical and mechanical properties of the bricks. The corresponding overall degradation of the graphite has to be evaluated to provide confidence in the continued safe operation of the plant.

Generally, the structural integrity of the nuclear graphite components is evaluated by irradiated material properties test data obtained from test reactors which are applied to a numerical or mathematical model [3]. On the other hand, relatively limited work has been reported for measurement of residual stress/strain in graphite. For example, by using acoustic emission (AE), Kasier [4] found that graphite emitted acoustic signal when it is stressed. He showed that by reloading the component AE could be detected only after the previous maximum stress had been exceeded; this phenomenon is called the Kaiser effect. Andrew [5] observed that graphite under stress emits noises which vary for different types of materials. Gilchrist and Wells [6] examined 2-in cubes of extruded graphite (isotropic and anisotropic). Kraus and Semmler [7] investigated graphite acoustic energy emission from small bending and tension stresses and they showed that the acoustic emission rate is higher during the first loading than the following load cycles. Neighbour and McEnaney [8] showed that AE responses from unirradiated nuclear graphites subject to cyclic loading exhibit the Felicity effect. This effect is the detection of AE before the previous maximum stress. They [9] also compared similar unirradiated and irradiated nuclear sleeve graphites in order to investigate reliability of the

technique for residual stress measurement. Overall it was concluded that AE monitoring is not a suitable technique for measuring internal stresses in irradiated graphite.

Indentation tests performed on the graphite for determination of the modulus of elasticity, also investigated the effects of local stresses and residual stresses. Oku [10] performed the micro-hardness tests on the six carbon materials to evaluate Young's modulus and bending strength of the samples from resulting hardness test load-displacement curves on the samples. Ishihara [11] estimated a relationship between hardness test data and residual strain using a model in which deformation receptivity is assumed to be proportional to the tangent of the stress-strain curve. By comparison Hartley [12] used blunt indentation on unoxidised and thermally oxidised IMI24 graphite to simulate local stress point acting on graphite moderator bricks.

There are very few methods for obtaining measurements of residual stresses deep within materials. One technique is deep hole drilling. It is a semi-invasive method for measurement of through thickness residual stresses. Initial studies by Zhdanov [13] and Beaney [14] were continued by Smith and co-workers to improve the technique. The method has been applied to metallic [15-21] and composite [22] materials. Recently, the versatility of the technique for measuring residual stress distributions in very thick components, components with difficult access to the measurement location and in-situ measurement for full-scale components has been reported by Kingston [23].

This paper considers the application of the DHD method for measuring residual stress through the thickness of the graphite components.

## NOMENCLATURE

| | |
|---|---|
| $E$ | Young's modulus |
| $M$ | Bending moment |
| $y$ | Distance of strain gauge to the neutral axis |
| $I$ | Area of moment of inertia |
| $b$, $h$ | Width and depth of the rectangular beams |
| $P$ | Measured load |
| $\varepsilon$ | Strain |
| $[M]$ | Compliance matrix |
| $[M]^*$ | Pseudo-Inverse of the matrix $[M]$ |
| $f[\theta,z]$, $g[\theta,z]$, $h[\theta,z]$, | Angular and through thickness functions |
| x,y | Co-ordinates in the plane normal to the axis of the reference hole |
| z | Position through thickness |
| $u_\theta$ | Reference hole hoop strain |
| $u_z$ | Reference hole through thickness strain |
| $\nu$ | Poisson's ratio |
| $\sigma_{xx}$, $\sigma_{yy}$ | Residual stresses on the plane normal to the axis of the reference hole |
| $\sigma_{zz}$ | Residual stresses parallel to the axis of the reference hole |
| $\hat{\sigma}$ | Vector of residual stresses |

## MATERIALS AND EXPERIMENTS

### Specimens

Two types of graphite were used, Pile Grade "A" (PGA) graphite and PG25 porous graphite. PGA samples were cut from blocks of material that had been used in an earlier programme by Holmes [24] as part of an investigation of mechanical behavior and ultrasonic measurement of graphite joints. PGA graphite has anisotropic material properties.

Rectangular specimens were extracted in directions parallel and perpendicular to the brick axis as shown schematically in Fig. 1. A rectangular bar of 190mm length with square section of 22mm depth and 23mm width was extracted parallel to the graphite brick axis. A further example of PGA graphite was a rectangular bar of length 190mm, depth 25mm and width 35mm. This was extracted from the same blocks but perpendicular to brick axis.

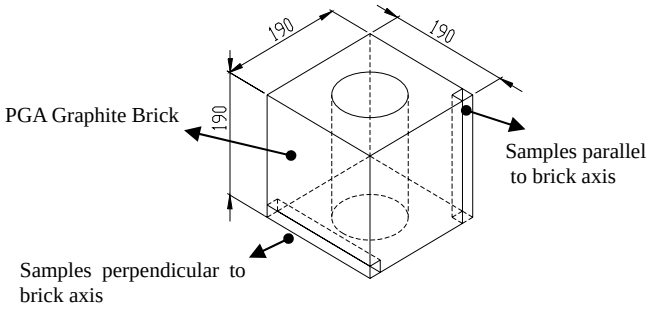


Fig.1. Direction of the samples of PGA graphite extracted from a brick, dimensions are in mm

PG25 porous graphite, with 48% porosity, was also examined to represent the high porosity in irradiated graphite. Rectangular beams of 180mm length, 25mm width and 35mm depth was extracted from rectangular blocks which were procured from Morganite Electrical Carbon. Typical material properties of PGA [25] and PG25 are shown in Table 1. Reported values for PG25 are provided by the manufacturer.

### Experiments

To evaluate the application of the DHD technique to the graphite samples, a four point bend rig was used to introduce a known stress distribution into the samples. This is shown schematically in Fig. 2 where the region between the two innermost rollers is subjected to a constant bending moment. This provides a tensile stress on the top surface and a compressive stress on the bottom surface of the beam. Hence, any reference hole introduced into the sample through its depth can be used to measure a linear stress distribution through the depth, h.

Prior to testing each sample a 3.18 mm diameter reference hole was machined into the centre of the beam with the axis of the reference hole parallel to the direction of loading as shown in Fig. 2. For each sample, two strain gauges were bonded on the top surface and two on the bottom. A summary of the samples tested is shown in Table 2.

Additional strain gauges were bonded on the sides of the beams to measure the variation of the strains through the cross section of the beam. Fig. 3 shows the location of strain gauges and the reference hole in the PGA sample cut perpendicular to brick axis. In order to determine the stresses applied to the beams it was necessary to determine the Young moduli of the samples. This was done by applying a known load to the rectangular specimens and reading strains from the strain gauges bonded to the samples. Loads were applied using a servo-electric test machine. Because of the low flexural and tensile strengths of the graphite samples loads were restricted.

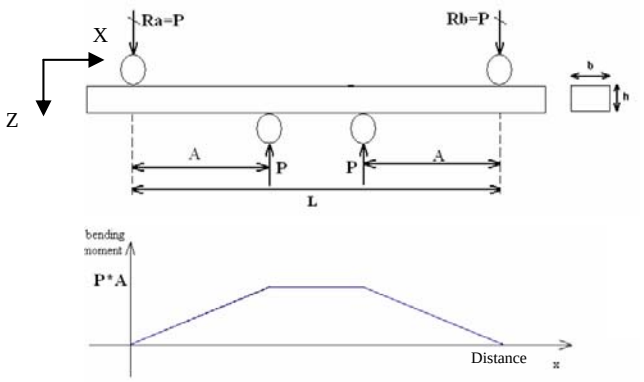


Fig.2. Loading condition in four-point bending test sample: A=50mm, L=150mm, b and h for each samples are presented in table 2

Values of $E$ were determined using simple beam bending theory, where

$$E = \frac{My}{I\varepsilon} \quad (1)$$

where $M$ is the bending moment, $y$ is the distance of the strain gauge to neutral axis, $I$ is the area moment of inertia, ε is the measured strain, $M$ and $I$ can be expressed as:

$$I = \frac{bh^3}{12} \quad (2)$$

$$M = PA \quad (3)$$

where $b$ is the width and $h$ is the depth of the rectangular cross section, $P$ is the measured load as illustrated in Fig. 2.

To undertake DHD measurements the four point bend rig had to be used away from a servo-electric test machine. Consequently, a screw mechanism was used to apply loads to the test rig and DHD measurements were undertaken.

There are four basic steps in the DHD method. First, bushes are glued on to surfaces of the sample for the entrance and exit points of the reference hole. A reference hole is drilled through the sample and the bushes. The hole diameter is measured using an air probe system, with measurements being taken at many points along the length of the hole and many angles. To release the stresses a core, containing the reference hole is trepanned and after trepanning the hole diameter is remeasured.

Table 1 Typical material properties of PGA graphite [25] and PG25

| Property | PGA-parallel to brick axis | PGA-perpendicular to brick axis | PG-25 |
|---|---|---|---|
| Bulk Density (Kg/m³) | 1678 | 1678 | 1080 |
| Compressive Strength (MPa) | 31±3.4 | 29.7±4.8 | 5.52 |
| Flexural Strength (MPa) | 18.3 | 12 | 2.76 |
| Tensile Strength (MPa) | 9.6±3.4 | 7.6±2.8 | 0.48 |

Table 2 Summary of the experiments

| Experiment No | Material | Specimen dimension (Length, width, depth) | Purpose |
|---|---|---|---|
| 1 | PGA graphite parallel to brick axis | 190x23x22 mm | Determination of E |
| 2 | PGA graphite perpendicular to brick axis | 190x35x25 mm | Determination of E |
| 3 | PG25 | 180x35x25 mm | Determination of E |
| 4,5,6 | PGA graphite parallel to brick axis | 190x23x22 mm | DHD measurement |
| 7,8 | PGA graphite perpendicular to brick axis | 190x35x25 mm | DHD measurement |
| 9 | PG25 | 180x35x25 mm | DHD measurement |

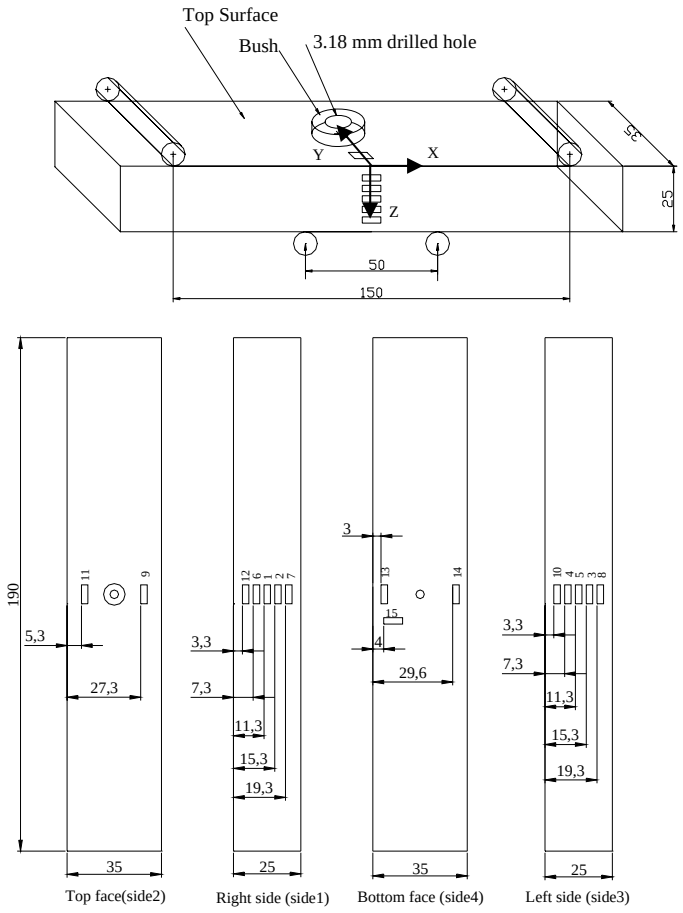


Fig. 3. Location of the strain gauges in the PGA sample perpendicular to brick axis, dimensions in mm.

The differences in hole diameter before and after trepanning are used to determine the initial stresses. Annex 1 describes the theory for determining the stresses from the measured distortions.

For the graphite beams the trepanning process was not undertaken. Instead the reference hole diameters were measured when the beams were loaded and unloaded. During loading, the strain gauges were monitored continuously using a data logging system. As will be seen later the normalised distortions were then compared with the strain gauge readings.

The PGA sample, cut parallel to the brick axis, was loaded in three steps and the diameters of the reference hole measured at each load step. Similar measurements were carried out in the PGA extracted from the perpendicular axis of the brick and also the PG25 sample.

## RESULTS

The experimentally determined values of *E* for PGA graphite are compared with reported values [24] in Table 3. Notably, the measured value in the parallel direction was greater then the quoted value for tension, while in the perpendicular direction the measured value was less than the quoted value. The measured value of *E* for PG25 graphite was 2GPa with an uncertainty of ±0.4GPa

Table 3 Measured and reported values [24] of *E* for the PGA graphite

| PGA graphite | Young's Modulus of PGA graphite | |
|---|---|---|
| | Parallel to Brick axis | Perpendicular to brick axis |
| Tension (reported) | 11.0±3.4GPa | 4.8±1.4GPa |
| Compression(reported) | 7.6±2.1GPa | 4.1±1.4GPa |
| Measured Values | 11.3±0.4GPa | 3.4±0.4GPa |

Typical results for measured hole distortions are shown in Fig 4. As expected, as shown in Fig 4 a) the reference hole in the top half of the beam (z=0 to 12.5mm) was in tensile and the lower half in compression. A typical angular hole distortion corresponding to a depth equal to 22mm, is shown in Figure 4b. The maximum strain occurred at θ = 90° and corresponded to the direction of the maximum principal stress in the beam.

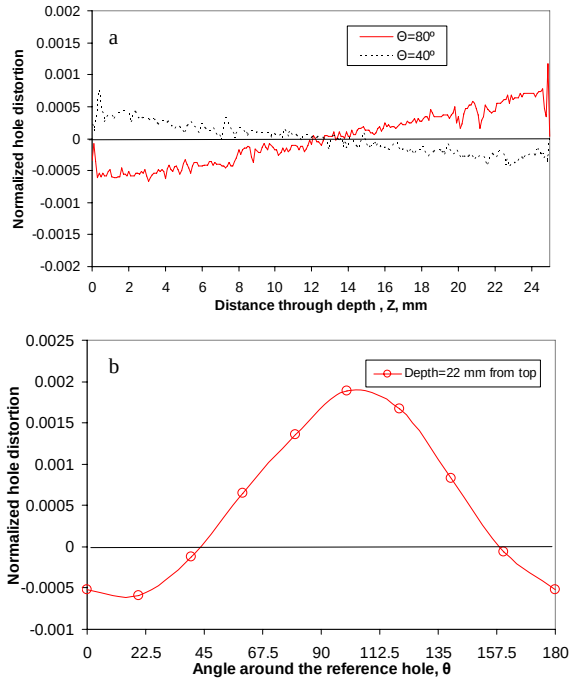


Fig. 4. Typical measured hole distortions resulted from DHD measurement a) Variation of through thickness strains b) Angular variation of the hole distortion

Figures 5 to 7 illustrate experimental results for strains determined from the measured reference hole distortions. Also shown are the strains measured on the surface of the graphite beams and in general it can be seen there is very good agreement between the two strain measurement methods. For example, Fig. 5 illustrates the strains determined at the first

load step and it is evident that through thickness strains less than 100 microstrain can be measured using the DHD method. Figure 6 illustrates a comparison between detailed surface strains and the through thickness distribution of strains obtained from the DHD measurements in a PGA sample. The agreement is very good. Figure 7 shows results obtained from the highly porous PG25 sample. The DHD through thickness strain measurements were much more noisy and only a reasonable agreement with the measured surface strains could be obtained by averaging through-thickness strains over intervals of 1mm. It is also noticeable that the surface strains shown in Figure 7 were not linear through the depth. Further work is being done to understand this.

The accuracy of the air-probe system was the main contributor to the measurement errors. This system has a displacement measurement accuracy of approximately ±0.5μm. The corresponding accuracy in stress measurement is proportional to Young's modulus. The error at each point shown in Fig 8 is about 0.27MPa and 0.15MPa in Fig 9.

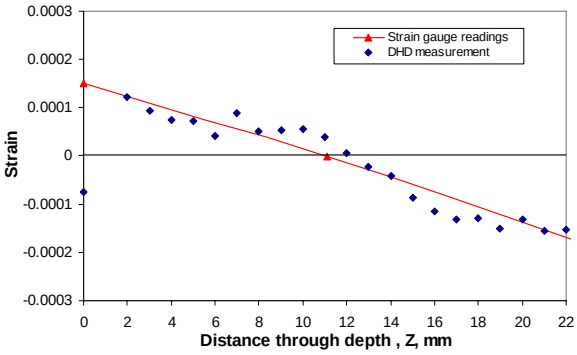


Fig. 5. DHD strains in the 1st loading step, PGA graphite beam extracted parallel to the brick axis

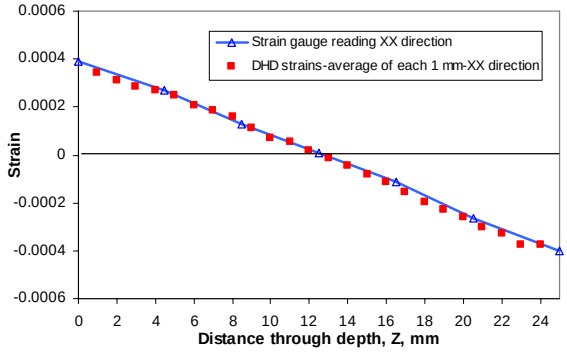


Fig. 6. Comparison between deep-hole drilling strains and strain gauge readings, PGA sample perpendicular to brick axis

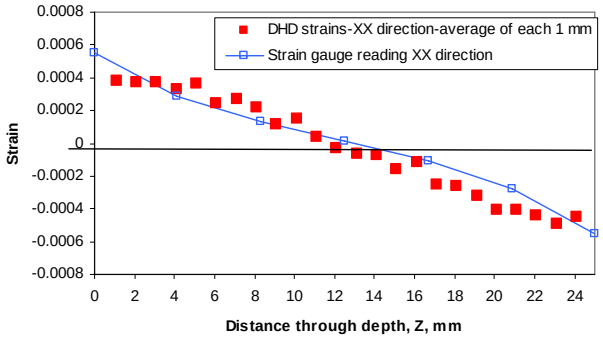


Fig. 7. Comparison between deep-hole drilling strains and strain gauge readings, PG25

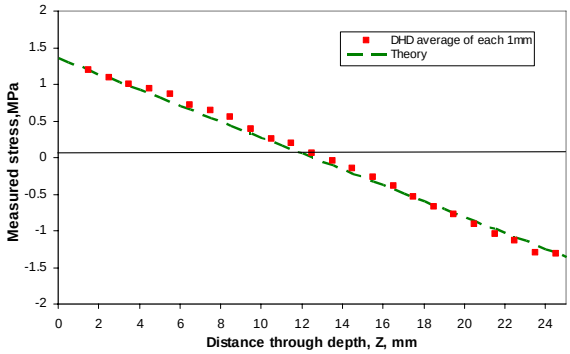


Fig. 8. Comparison between deep-hole drilling measured stress and theory, PGA sample perpendicular to brick axis

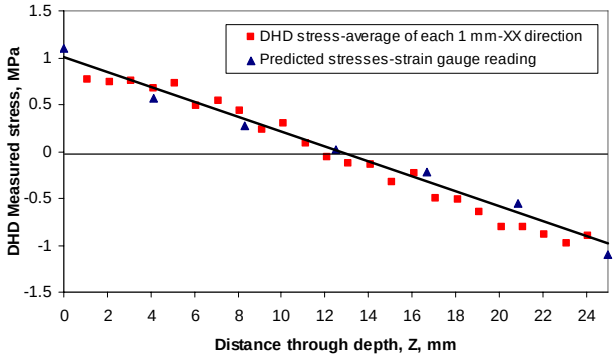


Fig. 9. DHD measured stress, PG25

## CONCLUDING REMARKS

In all experiments a linear through depth distribution of longitudinal strains was expected with tensile on the top surface and compressive on the bottom. The DHD method has been shown to provide a through thickness measurement of strains and stresses that agree well with external surface strain gauges. The results illustrate that the method is able to measure tensile and compressive strains over increments of 0.2mm through the depth. The sensitivity of the technique for measuring relatively low strains is shown by the results in Figs 5 and 6 for the PGA graphite. The corresponding stress distribution for the strain distribution shown in Fig 6 is illustrated in Fig 8 and demonstrates that stresses less than 1MPa were measured.

The porosity of PG25 graphite made the measurement strain sensitivity less compared to the more consolidated PGA graphite. Gauge lengths of 1mm through the depth had to be selected in order to obtain agreement with the surface measured strains. The through thickness stress distribution obtain via DHD measurements is shown in Fig 9. Similar to the PGA graphite stresses less than 1MPa were measured, although as Fig 9 illustrates the scatter in results was larger compared to the PGA graphite .

Further work is being conducted to determine the temperature sensitivity of the measurement technique. This is to assess its potential for in-reactor measurement of stress in graphite bricks.

## ACKNOWLEDGMENTS

This work was carried out as part of the TSEC programme KNOO and as such we are grateful to the EPSRC for funding under grant EP/C549465/1.

## REFERENCES

1. Bradford, M.R., *An overview of British Energy's graphite core assessment methodology.* Special publication - Royal Society of Chemistry, 2007. **309**: p. 19-24
2. Ellis, A.T. and K.M. Staples, *The management of Magnox graphite reactor cores to underwrite continued safe operation* Special publication- Royal Society of Chemistry, 2007. **309**: p. 3-10
3. Tsang, D.K.L. and B.J. Marsden, *The development of a stress analysis code for nuclear graphite components in gas-cooled reactors.* Journal of Nuclear Materials, 2006. **350**(3): p. 208-220.
4. Kaiser, J., *Untersuchung über das Auftreten von Geräuschen beim Zugversuch*, Dr.-Ing. Dissertation, Fakultät für Maschinenwesen und Elektrotechnik der Technischen Universität München (TUM); 15.2., 1950
5. Andrew, J.F., I. Okada, and D.C. Wobschall. *Elastic constants and permanent set in carbons and graphite at room temperature*. in *Proc. 4th Conf. Carbon*. 1960: Pergamon Press.
6. Gilchrist, K.E. and D. Wells, *Acoustic emission from graphite under stress.* Carbon, 1969. **7**(5): p. 627-631.
7. Kraus, G. and J. Semmler., *Determining the Mechanical Hardening of Carbon and Graphite Materials by Acoustic Emission Analysis(Die charakterisierung des mechanischenverhaltens von kohlenstoff- und graphitmaterialien mit hilfe der schallemissionsanalyse).* Carbon, 1978. **16**(3): p. 185-190
8. Neighbour, G.B. and B. McEnaney, *Creep and recovery in graphites at ambient temperature: An acoustic emission study.* Carbon, 1994. **32**(4): p. 553-558.
9. Neighbour, G.B. and B. McEnaney, *An investigation of acoustic emission from an irradiated nuclear graphite.* Journal of Nuclear Materials, 1995. **223**(3): p. 305-311.
10. Oku, T., S. Ota, and M. Tada. *Microhardness of graphite and C/C composite materials*. in *20th Biennial conference on carbon*. 1991. USA, CA.
11. Ishihara, M., S. Hanawa, T. Furusawa, J. Aihara, and Y. Tachibana. *Preliminary study on the development of an in-service inspection technique for graphite component* in *Technical commitee meeting on high temperature gas cooled reactors technology development*. 1996. South Africa.
12. Hartley, M. and B. McEnaney. *Blunt indentation of core graphite*. in *Specialist meeting on graphite moderator life cycle behaviour* 1995. Bath, United Kingdom: IAEA.
13. Zhdanov, I.M. and A.K. Gonchar, *Determining the residual welding stresses at a depth in metals.* Automatic Weld, 1978. **21**(9): p. 22-24. .
14. Beaney, E.M., Measurement of sub-surface stresses, 1980, CEGB Report, RD/B/N4325
15. Leggatt, R.H., D.J. Smith, S.D. Smith, and F. Faure, *Development and experimental validation of the deep hole method for residual stress measurement.* Journal of Strain Analysis for Engineering Design, 1996. **31**(3): p. 177-186.
16. Smith, D.J. and N.W. Bonner. *Measurement of residual stresses using the deep hole method*. 1996. Montreal, Can: ASME, New York, NY, USA.
17. George, D., E. Kingston, and D.J. Smith, *Residual stress measurement in thick section components.* American Society of Mechanical Engineers, Pressure Vessels and Piping Division (Publication) PVP, 2000. **410**: p. 275-278.
18. George, D. and D.J. Smith, *The application of the deep hole technique for measuring residual stresses in an autofrettaged tube.* American Society of Mechanical Engineers, Pressure Vessels and Piping Division (Publication) PVP, 2000. **406**: p. 25-28.
19. Smith, D., P. Bouchard, and D. George, *Measurement and prediction of residual stresses in thick-section steel welds.* The Journal of Strain Analysis for Engineering Design, 2000. **35**(4): p. 287-305.
20. George, D., E. Kingston, and D. Smith, *Measurement of through-thickness stresses using small holes.* The Journal of Strain Analysis for Engineering Design, 2002. **37**(2): p. 125-139.
21. George, D. and D.J. Smith, *Through thickness measurement of residual stresses in a stainless steel cylinder containing shallow and deep weld repairs.* International Journal of Pressure Vessels and Piping, 2005. **82**(4): p. 279-287.
22. Bateman, M.G., O.H. Miller, T.J. Palmer, C.E.P. Breen, E.J. Kingston, D.J. Smith, and M.J. Pavier,

 

*Measurement of residual stress in thick section composite laminates using the deep-hole method*. International Journal of Mechanical Sciences, 2005. **47**(11): p. 1718-1739.

23. Kingston, E.J., D. Stefanescu, A.H. Mahmoudi, C.E. Truman, and D.J. Smith, *Novel applications of the deep-hole drilling technique for measuring through-thickness residual stress distributions.* Journal of ASTM International, 2006. **3**(4).
24. Holmes, C., *The mechanical behaviour and ultrasonic measurement of graphite joints*, Mechanical Engineering, University of Bristol, 2003. **PhD**: p. 287
25. Warner, D.R.T., A review of PGA physical property data, 1984, CENG Report, SWR/SSD/0347/R84
26. Timoshenko.S and Goodier. J.N, *Theory of elasticity* 1951.

## ANNEX A

## MEASUREMENT ANALYSIS

Using measurement of the hole distortion between stressed and unstressed states, permits the DHD technique to measure internal stress distributions in a component. An analytical solution for the radial and tangential displacements around a hole in an infinite plate subjected to a far-field stress, Fig A1, can be written as: [26]

$$U_r = \frac{\sigma_0 a}{E}\left\{\left[(1+\nu)\frac{a}{2r}\right]+\left[(1-\nu)\frac{r}{2a}\right]+\left[(1-\nu)\frac{r}{2a}(1-\frac{a^4}{r^4})+\frac{2a}{r}\right]\cos 2\theta\right\}, \quad \text{(A1)}$$

$$U_\theta = -\frac{\sigma_0 r}{2E}\left[\left(1+\frac{a^2}{r^2}\right)^2+\nu\left(1-\frac{a^2}{r^2}\right)^2\right]\sin 2\theta, \quad \text{(A2)}$$

where $\sigma_0$ is the far-field applied stress, a is the radius of the hole, *E* is Young's modulus, ν Poisson's ratio and θ=0 is in the direction of the applied stress.

In the deep-hole drilling technique, radial distortion at the hole edge is measured; therefore, radial displacement at the edge of the hole can be calculated by substituting r=a in Eq.(A1)

$$u_r\Big|_{r=a} = \frac{\sigma_0 a}{E}(1+2\cos 2\theta) \quad \text{(A3)}$$

Normalized radial distortion at the edge of the hole can be defined as $\bar{u}$

$$\bar{u} = \frac{u_r|_{r=a}}{a} = \frac{\sigma_0}{E}(1+2\cos 2\theta) \quad \text{(A4)}$$

Eq. (A4) can be extended for far field biaxial stresses plus shear stresses in the form of:

$$\bar{u} = \frac{1}{E}\left[(1+2\cos 2\theta)\sigma_x + (1-2\cos 2\theta)\sigma_y + (4\sin 2\theta)\tau_{xy}\right] \quad \text{(A5)}$$

where the far field stresses are $\sigma_x, \sigma_y$, $\tau_{xy}$ and $\theta = 0$ is in the direction of the applied stress $\sigma_x$. The distortion must be measured at least at three different angles. Improved results can be obtained if the distortions are measured in the reference hole at m angles. A least squares fit to the measured distortions determines the initial stresses. For each through-thickness position z equation (A5) can be rewritten in matrix form as:

$$\bar{u} = [M]\bar{\sigma} \quad \text{(A6)}$$

where the measured hole distortion and stress vectors are:

$$\bar{u} = [u_\theta(\theta_1, z_1), u_\theta(\theta_2, z_1), ..., u_\theta(\theta_n, z_1), u_{zz}]^T$$

$$\hat{\sigma} = [\sigma_{xx}, \sigma_{yy}, \sigma_{zz}]^T$$

The compliance matrix *M* is given by

$$[M] = \frac{1}{E}\begin{bmatrix} f[\theta_1, z_1] & g[\theta_1, z_1] & h[\theta_1, z_1] \\ f[\theta_2, z_1] & g[\theta_2, z_1] & h[\theta_2, z_1] \\ . & . & . \\ . & . & . \\ . & . & . \\ f[\theta_n, z_1] & g[\theta_n, z_1] & h[\theta_n, z_1] \end{bmatrix}$$

therefore the optimum residual stress vector can be obtained by

$$\hat{\sigma} = [M]^* \hat{\varepsilon} \quad \text{(A7)}$$

where $[M]^* = (M^T M)^{-1} M^T$ is Pseudo-Inverse of the matrix *[M]*

The residual stress distribution through the thickness is obtained by using Eq (A7) at each measurement position z

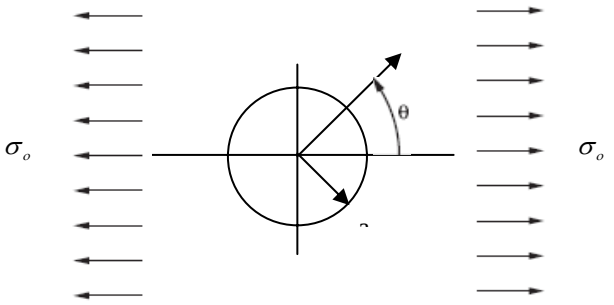


Fig. A1. Geometry of the hole subjected to far field stress $\sigma_0$